



Synthesis and Analysis of Novel Thermo-Acoustic and Mechanical Behaviour of Rattan Reinforced Composite for Value Added Applications

S Behera^{1,2}, J R Mohanty¹ & G Nath^{2*}

¹Department of Mechanical Engineering, Veer Surendra Sai University of Technology, Burla, Sambalpur, Odisha

²Department of Physics, Veer Surendra Sai University of Technology, Burla, Sambalpur, Odisha

Received 20 July 2022; revised 02 November 2022; accepted 08 November 2022

The idea of low cost green thermoacoustic composites urge special attention as an alternative candidate for synthetic composites in designing of sound proof and highly flexural components for pollution free electric vehicle and other automotive industries. Short randomly oriented rattan fiber has significant contribution in development of high strength to weight ratio composite with high frequency dispersion capability. The present work employs the hand layup method for synthesis followed by ultrasonic cavitation for surface treatment with compatible methanol blended acrylic acid. The Scanning-Electron-Microscopic (SEM) and Fourier Transform Infrared (FTIR) spectroscopic characterization confirmed the reorientation of different functional groups which facilitate the sound absorption and mechanical properties. The composite with admissible tensile strength 47.5 MPa and high flexural property 121.89 MPa along with 30 HV hardness value has quite distinguishable mechanical characteristics for the fabricated composites. The unique characteristic sound absorption feature of the rattan fiber composite supports the acoustic behaviour with sound absorption coefficient (SAC) of 97% classifies as Class-A type as per ASTM C423-17 standard. A continuous mass loss of 69% from 390.89°C to 475°C is well supported by thermo gravimetric analysis. The regression analysis provides the optimum mechanical performance for which the composites execute its accuracy. Low sound transmissibility of the composite enhances its acoustic performance. The thermo-acoustic insulating properties such as thermal conductivity and acoustic behaviour of the materials are well described converting the rattan fiber for sustainable and eco-friendly applications.

Keywords: Flexural components, Mechanical properties, Rattan fiber, Thermo-acoustic performance, Ultrasonic treatment

Introduction

The statistical data shared on the eve of an international event held at Stockholm with focal theme on “Human and Environment” highlighted that the hearing loss diseases of humans is expected to be increased to 25% on the globe by the year 2050. Thus, noise reduction is a challenging issue for future acousticians and environmentalists, which opens the relevant works on various noise reduction materials. Though the digital world very smartly engages synthetic and decorative materials for noise reduction, it further requires investigation on development of green acoustic material as an alternative potential candidate due to acute environmental issues associated with synthetic ones. Composites composed of abaca, flax, cornstalks, Date Palm Fibers, *Luffa cylindrica*, and hemp natural fiber are progressively replacing glass fiber usage in automotive body components for thermo-acoustic insulation, engine

shields, and so on.¹ To solve the growing issue of noise pollution, conventional materials such as synthetic fiber can be replaced by bio-material, which will provide additional advantages due to the many unique features without emitting any pollutant to open environment. Due to its potential to sound attenuation and its low weight, which leads to improved fuel efficiency, natural fiber-based composites are gaining popularity, particularly in the automotive industry.² Though there are many works^{3,4} related to sound-absorbing material based on natural fibers, but as a new species, rattan fiber (RF) has novelty in development of acoustic material due to its special features such as durability and resistance to splintering nature. Rattan fiber's lower density than synthetic fiber and relative low density compared to other natural fibers is the primary factor in the decreased weight of polymer composites composed of rattan fibers. Rattan fiber also has a greater specific strength. Rattan fiber based polymer composites have higher specific mechanical properties, such as specific tensile strength and

*Author for Correspondence
E-mail: ganeswar.nath@gmail.com

specific modulus, due to the combination of the above two rare qualities of rattan fiber. This can be a potential material in EVs by reducing power requirement needed due to its higher strength to weight ratio also lowers the energy and cost needed for its manufacturing.^{5,6} There are many recommended work³⁻¹² on different natural fiber based acoustic materials which confirms there is almost no work on acoustic performance of rattan fibers, which is considered as special material in the present work. Detailed literature surveys on development of the composite materials using rattan as reinforcement are summarized in Table 1.

Materials and Methods

Synthesis of TRF/Epoxy Composite

Rattan plant stem (RPS) (Calamoideae) collected from the local area are cut into 25–30 cm in length, after which it was soaked in water for 1 month to allow microbial degradation, which separates the cellular tissue and pectin that surrounds the fiber bundles. Then long fibers are extracted from RPS and allowed to dry in an oven for 24 hr at 100°C to remove moistures present on the fiber surface. Then the long rattan fibers are converted into short rattan fibers of 1–3 mm in length. The methanol blended acrylic acid compatible solvent mixture prepared by ultrasonic interferometry technique was used for surface treatment, and here the fibers are termed as treat rattan fiber (TRF). Epoxy resin of grade LY-556 and Hardener of grade HY-951 which are brought from CF-Composites, New Delhi, are mixed at 10:1 ratio as recommended by the manufacturer. Then TRF was mixed with prepared resin and stirred with the help of a mechanical stirrer. Compression molding technique was used for the synthesis of TRF/Epoxy composite.¹⁷ The detailed fabrication process of rattan

fiber composite is given in Fig. 1. The prepared TRF/Epoxy composite were then machined to various shapes as per the analysis requirement.

Characterization of TRF/Epoxy Composite

Surface morphological analysis of TRF and TRF/Epoxy composites were performed with Scanning-Electron-Microscope (SEM) Quanta-FEG 650 (QEMSCAN F.E.I, Netherland) at accelerating voltage of 20 kV. Before conducting the surface analysis, the samples were dried in an oven to remove if any moisture present and were cut into slices. These samples were coated with carbon to make them conducting and finally placed on an aluminium stump holder by using a double sided tape to capture clear pictures of TRF/Epoxy composite microstructure.¹⁸ Energy Dispersive Spectra (EDS) of microstructure have been implemented to obtain elements present in the TRF/Epoxy material.¹⁹ Fourier Transform Infrared Spectroscopy (FTIR) spectra of TRF/Epoxy composite were carried out in the range of 4000–

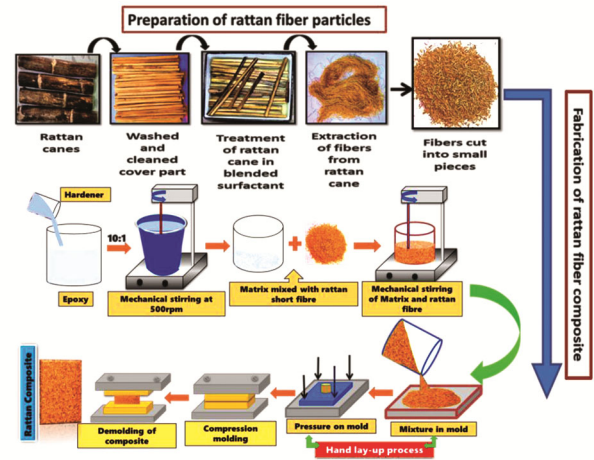


Fig. 1 — Detailed fabrication process of rattan fiber composite

Table 1 — Summary of recent different works on rattan fiber based composite materials and their characteristic

Year ^(Ref. No.)	Fiber	Treatment	Characterization	Physical property	Mechanical property	Thermal Property	Acoustic Property
2021 ⁽⁷⁾	Rattan	Deionized water	√√	××	√√	√√	××
2021 ⁽⁸⁾	Rattan	××	√√	√√	√√	××	××
2020 ⁽⁹⁾	Rattan	90% alcohol	××	××	√√	××	××
2019 ⁽¹⁰⁾	Rattan	15% NaOH	××	××	√√	××	××
	Banana						
2018 ⁽¹¹⁾	Rattan	5% alkylation	√√	××	√√	××	××
2018 ⁽¹²⁾	Rattan	NaOH	××	√√	√√	××	××
2018 ⁽¹³⁾	Rattan	××	××	××	√√	××	××
2017 ⁽¹⁴⁾	Rattan	××	√√	√√	√√	√√	××
2022 ⁽¹⁵⁾	Rattan	NaOH	√√	√√	√√	××	××
2015 ⁽¹⁶⁾	Rattan	KOH	××	√√	××	××	××

600 cm^{-1} using a thermo-scientific Spectrophotometer (Nicolet 6700) to the different functional groups present on the composite.²⁰ The samples have been taken in powder form and prepared into pellets by using KBr powder. For thermo gravimetric (TGA) and differential scanning spectroscopy (DSC) analysis of TRF composite, 6 mg of test sample were used, and experiment was carried out using PerkinElmer STA-8000 equipment as per ASTM E1269.01 standardization. The experiment was done at a constant heat rate of 10 $^{\circ}\text{C}/\text{min}$ with a limited temperature at 30 to 800 $^{\circ}\text{C}$.

Mechanical Testing of TRF/Epoxy Composite

Tensile Testing of the TRF/Epoxy Composite

Tensile properties measurements were carried out utilising a Universal Testing Machine (UTM) INSTRON series 3382 with a 5 kN load cell. Dumbbell shaped ASTM D 638 standard specimens were machined. Five different samples with varying fiber concentration, i.e., 5, 10, 15, 20, and 25 wt. % were examined with moving cross head speed of 2 $\text{mm}\cdot\text{min}^{-1}$. The temperature of the testing room was maintained at 23 $^{\circ}\text{C}$ with humidity level of 54%. The average tensile value was calculated and plotted.

Determination of Optimum Weight Percentage of TRF/Epoxy Composite

The tensile strength of the composite has been plotted for different wt. % of TRF as shown in Fig. 2. The strength of fibers increases with the rise of fiber percentages and decreases after a particular wt. %.²¹ The experimental results for the tensile strength data of TRF/Epoxy composite were fitted with wt. % of TRF by a second-degree polynomial to establish the statistical relationship between tensile strength and fiber loading in order to obtain the best wt. % of fiber. Curve $y = -0.09x^2 + 3.2995x + 13.49$ with a coefficient of correlation (R^2 -value) of 0.9688 gives

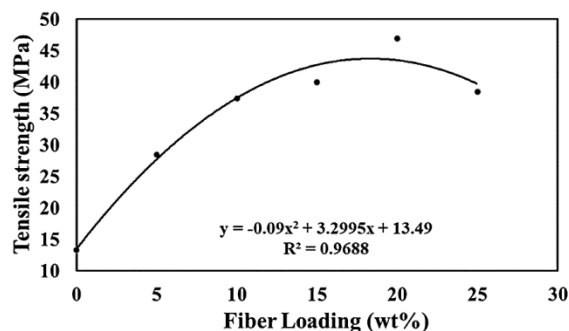


Fig. 2 — Second degree polynomial regression analysis of tensile strength with fiber loading

the maximum tensile strength at 18 wt. % of fiber loading. Regression analysis data for the optimum wt. % of TRF leads to the other characteristics analysis supporting the composite material.

Flexural Testing of the TRF/Epoxy Composite

Three points bending flexural testing were conducted for TRF/Epoxy composite specimen using servo-hydraulic 100 kN capable load cell INSTRON 3382 UTM. The fabricated samples were machined into $127 \times 12.7 \times 3.2 \text{ mm}^3$ dimension as per ASTM D790-99 standard and mounted on the machine as shown in Fig. 2. A total of five samples were examined for each fiber loading (i.e., 0, 5, 10, 15, 18, 20, 25 wt. %) and the average value were considered for accurate results. All the tests were performed in a controlled atmosphere of 23 $^{\circ}\text{C}$ temperature and 55% humidity level. The flexural testing arrangement is shown in Fig. 3.

Hardness Testing of TRF/Epoxy Composite

The micro hardness of TRF/Epoxy composite having specimen size of $50 \times 50 \text{ cm}^2$ has been obtained using Vickers's hardness tester as per ASTM E 384 standard at a load of 80 g and dwell time of 10 s.²² The reading has been taken in three different locations with an error bar. For each composition, five test specimens were tested and average values have been calculated.

Experimental Setup for Acoustic Measurement

Sound absorption (α) and sound transmission loss (TL_n) of the TRF/Epoxy composite was evaluated using impedance tube (Holmarc Opto-Mechatronics Pvt.-Ltd) of model ED-A-03 type. Transfer-function

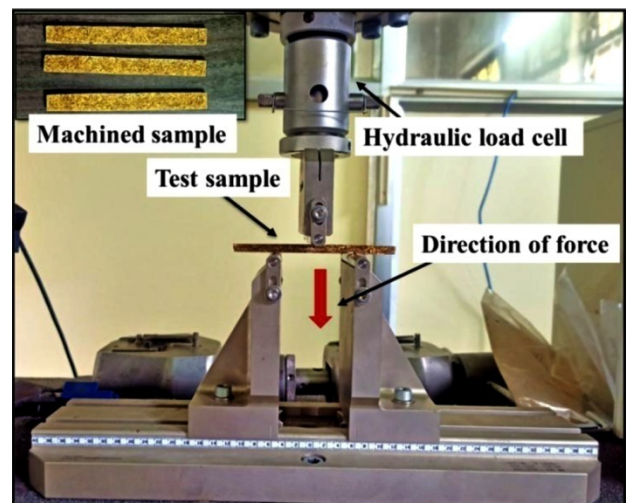


Fig. 3 — Three point bending flexural test arrangement

based measurement method at 0° normal incident according to ISO10534-2 is used. For absorption coefficient international standards ASTM E1050 and ASTM E2611 for transmission loss is used to measure the required sound properties under 1/3 octave frequency ranges of 500–3150 Hz. For measurements of absorption coefficient, the test sample of 50 mm diameter has been inside at one of the ends of anodized tube of aluminium with a rigid backing while at the other end, a sound source is present which is powered by a signal generator. As the sound wave is generated by a complex electrical wave, its interaction with the material will produce a harmonic motion of the particles of the medium, that oscillates with frequency of the sound wave based on which the transfer function absorption coefficients are computed using the data acquisition.²³ In order to measure the sound transmission loss (STL), the impedance tube has been used. The impedance tube is equipped with a hollow aluminium tube behaving as an anechoic chamber. Wave Analyser 4C software has been used to record the data. Measurement data were recorded for composite specimens with various weight percentage of the rattan fiber. The complete experimental setup for sound absorption and sound transmission loss tests is shown in Fig. 4.

Experimental Setup for Thermal Conductivity

The thermal conductivity measurements (Fig. 5) were carried out according to ASTM D5334-14 standard by TEMPOS thermal properties analyser using a TR-3 sensor which is 100 mm in length and 2.4 mm in diameter is suitable for soft porous composite materials.²³ For each composition (i.e., 0, 5, 10, 15, 20 and 25 wt. % fiber loading), the measurement has been performed five times and the average values have been recorded.

Results and Discussion

From Fig. 6 the surface morphology of Untreated Fiber (UF), acrylic acid TRF, and TRF/Epoxy composite could be seen. As observed from Fig. 6(a), the surface structure of UF is smooth due to the existence of impurities, lignin, pectin, and waxy substances, which cause the fiber to become hydrophilic.²⁴ Compared with UF, Fig. 6(b) shows that after acrylic acid blending, the surface texture of rattan fiber becomes rough and uneven. The treatment causes removal of impurities such as fatty acids, waxes, lignin, and adhesive pectin, creating tiny holes, air cavities, and pits on the rattan fiber surface.

Due to fibrillation, the fiber-matrix adhesion increases followed by hydrophobicity nature of the TRF.²⁵

With increase of air cavities on the fiber's surface, the fiber becomes more porous, enabling them to be good sound absorber.²⁶ The morphology of TRF/Epoxy composite which contains a lot of pores of closed and open in nature could be seen in Fig. 6 (c). The presence of open pores creates a communication channel while the closed pores increase the bulk density, mechanical strength, and thermal conductivity converting the composite to become more suitable for guiding of the sound wave through it. The EDS of TRF/Epoxy composite was

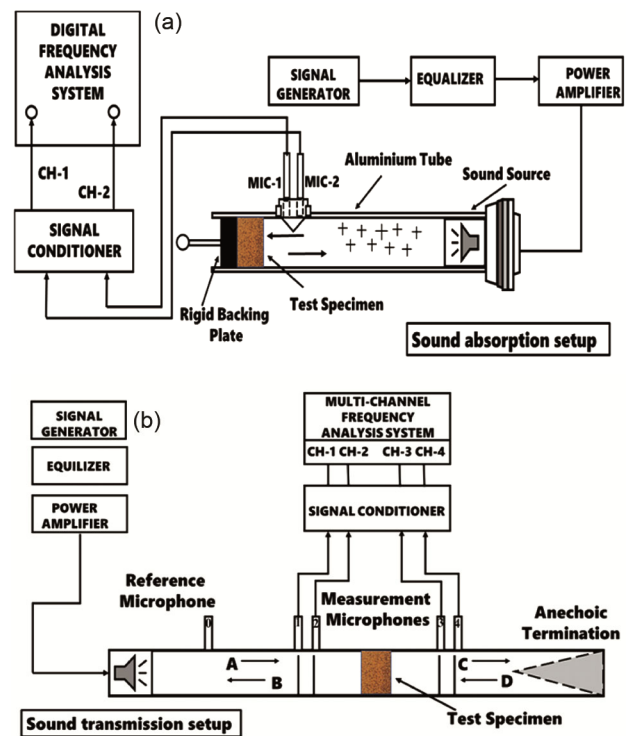


Fig. 4 — Setup of (a) sound absorption (α), (b) sound transmission loss (TLn)

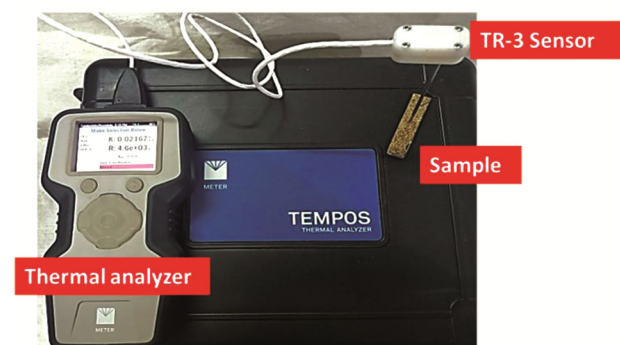


Fig. 5 — Thermal conductivity measurement testing arrangement

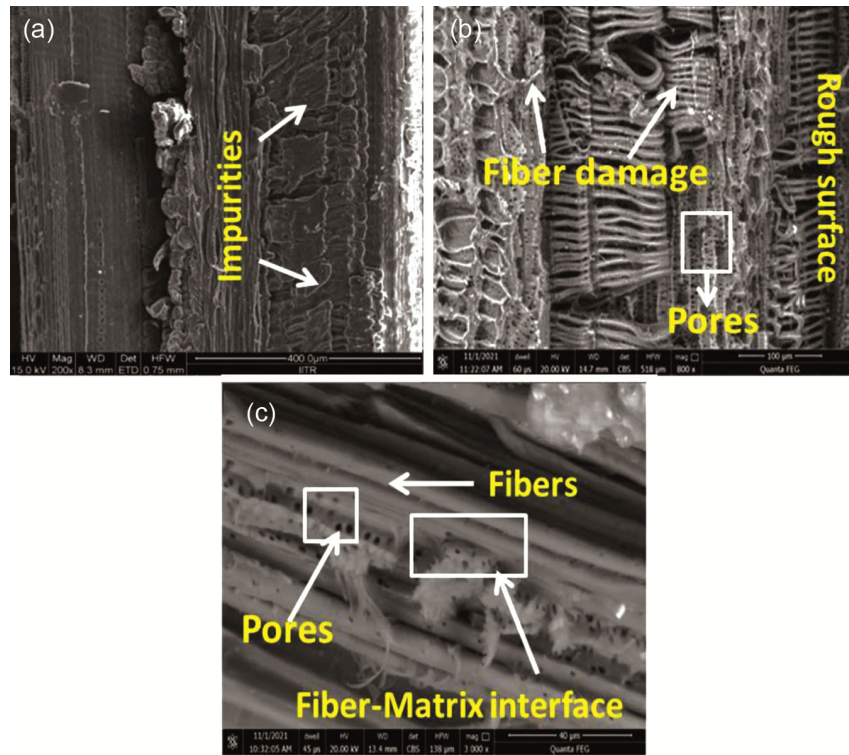


Fig. 6 — SEM micrograph of (a) untreated rattan fiber (b) treated rattan fiber (c) TRF/Epoxy composite

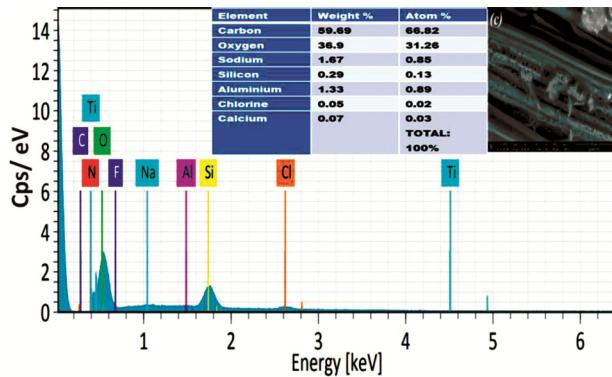


Fig. 7 — Elemental analysis of TRF/Epoxy composite

performed for quantitative elemental analysis. The energy spectrum in Fig. 7 displays different elemental peaks and their atomic weight percentages present in the material. The TRF/Epoxy composite consists of elements such as carbon, oxygen, sodium, silicon, aluminium, chlorine, and calcium. The result shows that the main constituents of TRF/Epoxy composite are carbon and oxygen which are due to presence of cellulose, hemicellulose, lignin, and waxes in Rattan fiber. The oxygen that exists on the material surface may build hydroxyl bonds with the hydrogen in the cellulose content, attracting more moisture and weakening the composite's strength. Existence of sodium is because of the acrylic acid surface

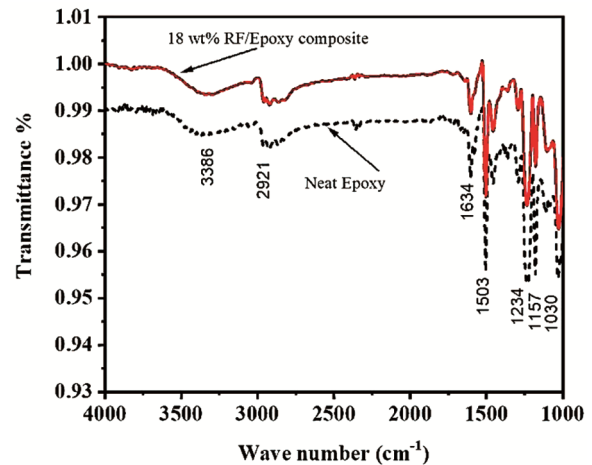


Fig. 8 — FTIR spectroscopy of TRF/Epoxy composite

modification of the fiber. Small quantity of minerals such as silicon, chlorine, aluminium, calcium was also found. Presence of high amount of oxygen i.e., 36.9% might be due to oxygen filled porous structure of fibrous composite material.^{27,28}

Using FTIR spectroscopy the microscopic changes in different functional group which constitutes the rattan fiber composite has been observed. The deformations occurring at functional group cellulose are shown in Fig. 8 with respect to transmittance % and the wave number. Each wave number is assigned

to a special bonding or stretching with increase in IR transmittance %. From the IR spectrum band, it is clearly observed that the broad band has occurred at 3386 cm^{-1} . In both cases the band is similarly stretched indicating that there is not much deformation in -OH group. But nearly around 3859 cm^{-1} the composite shows a higher band length than epoxy. This may be due to the removal of hydroxyl group of the cellulose due to chemical treatment of rattan fiber.²⁹ A huge energy band is observed from 2921 cm^{-1} to 1634 cm^{-1} in both epoxy and composite indicating the vibration of α -keto carbonyl group of cellulose. In the spectrum there is an unusual behaviour of functional group observed at wave number 2346 cm^{-1} that is attributed to presence of nitrile and alkyne clusters of cellulose which puts very less impact in the cellulose deformation. From 1634 to 1324 cm^{-1} the rattan composite shows C=O stretching of lignin and removal of lignin components from the fiber surface due to action of methanol blended acrylic acid. The deserted bands from 1503 to 1030 cm^{-1} in rattan fiber are of short band length than the raw epoxy due to the more ring side vibration of C-O-H groups of lignin and C-O-R (glycoside) groups of hemicellulose.³⁰ Thus, the action of surfactants on the surface of rattan fiber suitably modifies the functional group of the lignocellulosic components for enhancement of sound absorption.

The flexural behaviour of short random oriented TRF/Epoxy composite at various weight fractions is shown in Fig. 9. The average value of flexural strengths observed to be increased gradually from 55.02 MPa for neat thermosetting epoxy attaining maximum value of 121.89 MPa at 18 wt. %. With

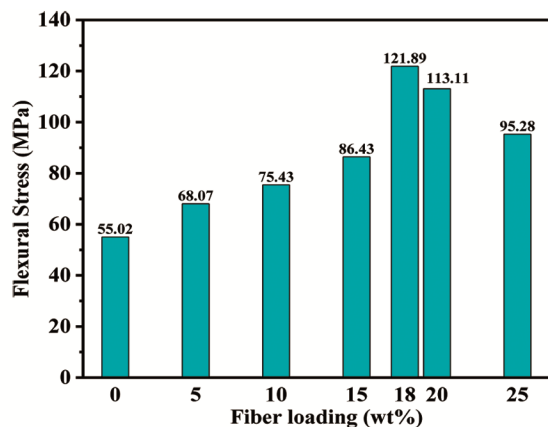


Fig. 9 — Flexural strength of TRF/Epoxy composite with varying fiber loading

increasing fiber loading increase in strength is due to strong interfacial adhesion between fiber and matrix, which is strengthened by chemical modification of fiber. Beyond 18 wt. % fiber loading, flexural strength reduces due to insufficient filling of matrix. The flexure strength of TRF/Epoxy composite is computed by the Eq. (1).³¹

$$\sigma_f = \frac{3WL}{2bt^2} \quad \dots (1)$$

where, W is maximum load, L = effective span length of test specimen, b = breadth of test specimen, and t = thickness of test specimen.

The experimental results of flexural stress in MPa Vs flexural strain (%) at various short TRF concentrations is shown in Fig. 10. A linear increasing flexural behaviour is observed by all the composites. With the increment of TRF content the bending ability of composite increases up to certain percentages due to exceptional stiffness of rattan fiber. At the end of linear stress-strain behaviour a sudden fall at the end in stress due to brittle rupture of composites. Similar trend is also noticed in Cordia-dichotoma reinforced fiber epoxy composite.²⁷ Flexure strain is determined by Eq. (2).⁽³¹⁾

$$\varepsilon = \frac{6\delta t}{b^2} \quad \dots (2)$$

where, ε flexure is strain of TRF/Epoxy composite and δ is the bending deflection given by the expression $\delta = \frac{WL^3}{48EI}$, EI is the rigidity modulus of specimen.

The evaluated micro-hardness value with error bars of fabricated composite with varying weight fractions of TRF is shown in Fig. 11. It is noted that the hardness value of composite increases with incorporation of TRF, and with increasing fiber content remarkable increase in hardness value is observed. This may be due to distribution of TRF in the matrix, which provides more robust cross-linking. After reaching a certain quantity of TRF, hardness

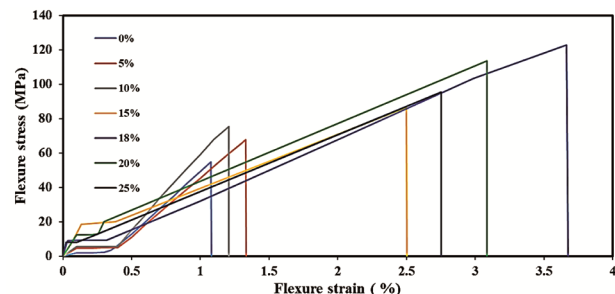


Fig. 10 — Flexure stress-strain plot for TRF/Epoxy composite at different fiber loading

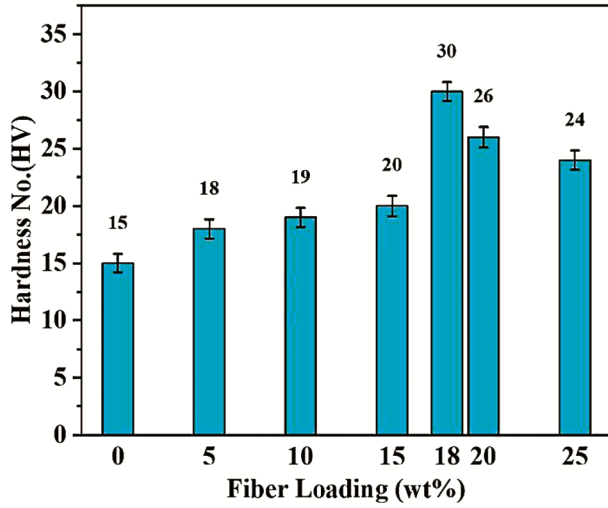


Fig. 11 — Micro hardness of TR F/Epoxy composite at varying fiber loading

value decreases due to an insufficient amount of matrix, leading to poor interfacial adhesion.

The sound absorption behaviour of test specimens was investigated using a standard impedance tube method at a 1/3 octave frequency band in the range of 500–3150 Hz. From Fig. 12 (a), it was observed that the SAC was comparatively lower at 500 Hz and then increases significantly attaining a maximum at about 1000 Hz after which it further increases at higher frequencies followed by sharp decrease in the frequency range 1500–2500 Hz as observed in the literature.³² SAC curves were found to follow a similar trend for all weight percentages of TRF/Epoxy composite, with the peak value of α at 1000 Hz. The modified TRF are free from cellulosic materials creating active sites with increasing surface area for an enhanced fiber and matrix interlock. The main mechanism behind the dispersion of sound energy in fibrous material is basically may be due to (i) When a sound wave hits the porous composite materials, it causes air particles to vibrate, causing internal friction between air particles and porous fibrous walls, producing viscous effects and converts non-conservative sound energy into conservative heat energy. (ii) Density difference between air particles inside the pores promotes temperature distinction which results, dissipation of energy during this process and finally (iii) Oscillatory movement of air inside the sample also transforms sound energy into mechanical energy.³³ The variation of sound absorption coefficient with fiber weight fraction shows a significant effect of wt% of fiber content as

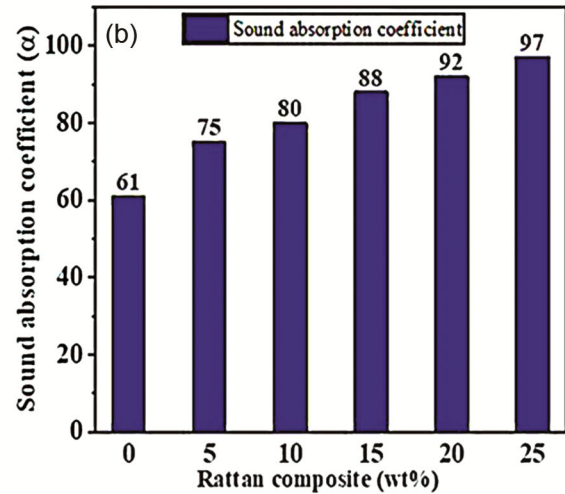
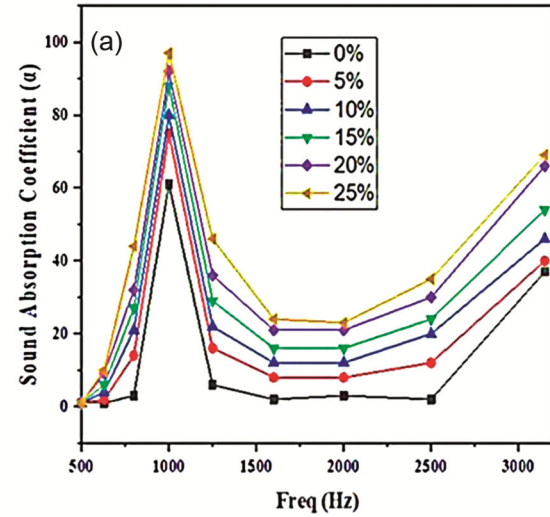


Fig. 12 — Sound absorption coefficient of TRF/Epoxy composite with (a) varying frequency (b) varying fiber loading

shown in Fig. 12b. With increasing weight fraction of fiber in the matrix, the SAC increases. SAC of neat epoxy is 0.61, whereas 25% of TRF/Epoxy composite possess ultimate sound absorption coefficient, i.e., 0.97 with approximately 47% increment as per ASTM C423-17 standardization, this bio-material may be classified as a most efficient sound absorber of class-A.

Sound transmission loss increases as observed from the Fig. 13 with increasing fiber loading from 5% to 25% and the lowest value has been obtained for pure epoxy polymer. The relation between STL and mass of composite is given in Eq. (3).⁽³⁴⁾

$$TLn = 20 \log (f \times m) - 47.3 \quad \dots (3)$$

where, TLn is sound transmission loss in dB, f is frequency in Hz, m is mass density of composite

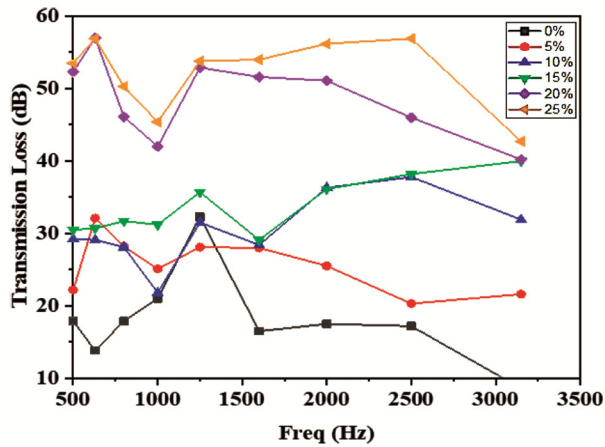


Fig. 13 — Transmission loss vs frequency of TRF/Epoxy composite

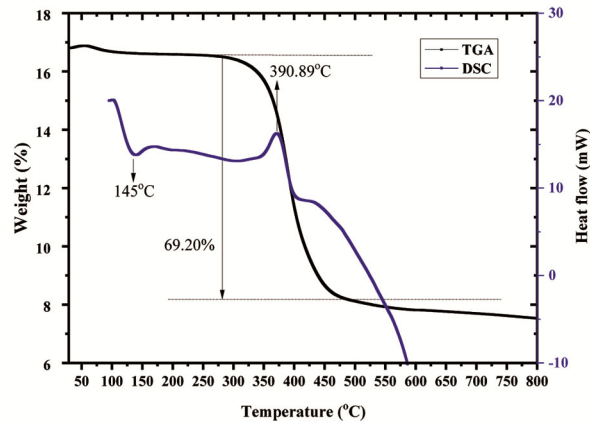


Fig. 14 — Thermo gravimetric analysis and Differential Scanning Spectroscopy of TRF/Epoxy composite

materials in kg/m^2 and 47.3 is a numerical constant in decibel. From Eq. (3), it is clear that the barrier composite transmission loss increases with increasing weight percentage. As the density of fiber is lower than the density of matrix, thus with increasing weight fraction, the density of composite decreases leading to anomalous behaviour in transmission loss.³⁵

The thermogram curve of TRF/Epoxy composite is shown in Fig. 14. It is observed that single step thermal decomposition occurs in the TRF/Epoxy composite where no significant mass change occurs from 30 to 270°C. The procedural breakdown or decomposition starts at 270°C with 69.2% mass loss of TRF/Epoxy composite being completed at 489°C. Degradation between 270°C to 390°C corresponds to gaseous breakdown of the TRF/Epoxy composite.³⁶ This is primarily due to elimination of the hemicellulose and pectin of TRF. The thermogram of TRF/Epoxy composite shows that the incorporation of

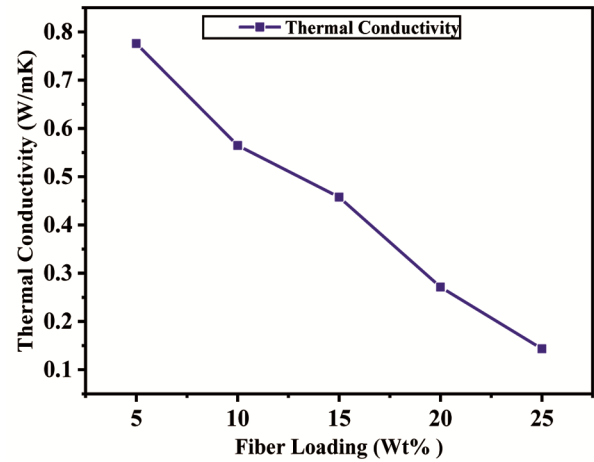


Fig. 15 — Thermal conductivity of TRF/Epoxy composite at various fiber loading

TRF in epoxy resin maintains sustainability of composite material up to 270°C. Thus, the TRF/Epoxy composite can be employed in application where operating temperature is less than 270°C. An exothermic peak at the temperature range 30 to 145°C is observed due to the vaporization of water.³⁷ An endothermic peak at 390.89°C indicates melting temperature TRF/Epoxy composite.³⁸ Thus, fabricated TRF/Epoxy composite can uphold its structural integrity up to 390°C.

The random orientation of short TRF within the disorganized polymer-chains results in poor transfer of thermal energy within the composite materials. The ability of composite materials to conduct thermal energy decreases after 0.07758 to 0.01433 W/mK with increase in fiber content in the composites happening from 5 to 25%, as shown in the Fig. 15. TRF/Epoxy composite with 25% fiber loading show lowest thermal conductivity of 0.01433 W/mK caused by low atomic density, poor binding energy and high anharmonicity in molecular vibration.

The thermal conductivity of composite materials mainly depends upon types of fillers, shapes, sizes, and complex crystal structure. Heat diffusion mechanism in most polymers is phonon transfer with each sub-atomic particle. With increase of natural fiber content which have low heat transfer property, the number of voids and lattice imperfections increases, introducing anharmonicity resulting in phonon scattering. As the heat wave incidents on the surface atoms and transfers to adjustment atoms, it will not be able to propagate properly due to disordered vibration of atoms causing slow heat diffusion.³⁹ Again, as phonon propagates with

increasing fiber content, number of interfaces increases resulting in more scattering. Polymers are thermal insulators, and by incorporating eco-friendly TRF from 5 to 25%, the thermal conductivity decreases approximately 5.40 times, making it an even more thermally insulating material.

Conclusions

With the aid of ultrasonic treatment rattan fibers are well modified for suitability of fabrication of composites with large number of interfacial sites for linking of small fibers. The pores of different shape having open and closed nature are well developed confirmed by SEM and appearing of various functional groups studied by FTIR supports the acoustic behaviour. The regression analysis shows that 18 wt. % of fiber loading provides the optimum mechanical performance at which almost all the characteristic features of the composite show unique behaviour in different physical properties. At optimum fiber loading, the maximum tensile strength, flexural strength, and hardness of TRF/Epoxy composite are 47.5 MPa, 121.89 MPa, and 30 HV, respectively. This TRF/Epoxy composite can also be employed in automotive applications due to its high flexural strength. The low thermal conductivity and high biodegradability executed by the composites has unique features for various applications in designing of different flexible and thermal insulating structure for automotive industries and designing of thermo-acoustic proof material in civil construction. Further, high transmission loss of the fabricated composite mostly provides the best application in wall and other components of sophisticated buildings in metropolitan cities and acute noise probe regions.

Reference

- Milan S, Christopher T, Manivannan A, Mayandi K & Winowlin Jappes J T, Mechanical and thermal properties of a novel *Spinifex littoreus* fiber reinforced polymer composites as an alternate for synthetic glass fiber composites, *Mater Res Express*, **8** (2021) 035301.
- Billah M M, Rabbi M S & Hasan A, A review on developments in manufacturing process and mechanical properties of natural fiber composites, *J Eng Adv*, **2** (2021) 13–23.
- Ramamoorthy M & Rengasamy R S, Study on the effects of denier and shapes of polyester fibers on acoustic performance of needle-punched nonwovens with air-gap: comparison of artificial neural network and regression modelling approaches to predict the sound absorption coefficient of nonwovens, *J Text Inst*, **110** (2019) 1–9.
- Hassani P, Soltani P, Ghane M & Zarrebini M, Porous resin-bonded recycled denim composite as an efficient sound-absorbing material, *Appl Acous*, **173** (2021) 107710.
- Billah M M, Rabbi M S & Hasan A, Injection molded discontinuous and continuous rattan fiber reinforced polypropylene composite: Development, experimental and analytical investigations, *Results Mater*, **13** (2022) 100261.
- Ding L, Han X, Cao L, Chen Y, Ling Z, Han J, He S & Jiang S, Characterization of natural fiber from manau rattan (*Calamus manan*) as a potential reinforcement for polymer-based composites, *J Bioresour Bioprod*, **7** (2022) 190–200.
- Gholampour A & Ozbakkaloglu T, A review of natural fiber composites: properties, modification and processing techniques, characterization, applications, *J Mater Sci*, **55** (2020) 829–892.
- Vigneshwaran S, Sundarakannan R, John K M, Joel Johnson R D, Prasath K A, Ajith S, Arumugaprabu V & Uthayakumar M, Recent advancement in the natural fiber polymer composites: A comprehensive review, *J Clean Prod*, **277** (2020) 124109.
- Berardi U & Iannace G, Acoustic characterization of natural fibers for sound absorption applications, *Build Environ*, **94** (2015) 840–852.
- Singh P P & Nath G, Development of sustainable thermo acoustic material from residual organic wastes, *J Sci Ind Res*, **81(3)** (2022) 215–225.
- Liu X, Wang R, Tian G, Yang S, Wang Y & Jiang Z, Tensile properties of single rattan fibers, *Wood Sci Technol*, **46** (2014) 519–526.
- Joshi M, Charles B, Ravikanth G & Aravind N A, Assigning conservation value and identifying hotspots of endemic rattan diversity in the Western Ghats, India, *Plant Divers*, **39** (2017) 263–272.
- Belcher B, Imang N & Achdiawan R, Rattan, rubber or oil palm: Cultural and financial considerations for farmers in Kalimantan, *Econ Bot*, **58** (2004) 77–87.
- Shaanker R U, *Bamboos and Rattans of the Western Ghats: Population Biology, Socio-Economics and Conservation Strategies* (Ashoka Trust for Research in Ecology and the Environment) 2004.
- Singh P P & Nath G, Ultrasonic processing and thermo-acoustic analysis of orange peel waste as smart acoustic material: Waste and biomass valorization, *Waste Biomass Valor*, **13** (2022) 2905–2916.
- Li M, Pu Y, Thomas V M, Yoo C G, Ozcan S, Deng Y, Nelson K & Ragauskas A J, Recent advancements of plant-based natural fiber-reinforced composites and their applications, *Compos B Eng*, **200** (2020) 108254.
- Jain J & Sinha S, Potential of pineapple leaf fibers and their modifications for development of tile composites, *J Nat Fibers*, **1** (2021) 4822–4834.
- Nayak S & Mohanty J R, Influence of chemical treatment on tensile strength, water absorption, surface morphology, and thermal analysis of Areca sheath fibers, *J Nat Fibers*, **16** (2019) 589–599.
- Cao L, Fu Q, Si Y, Ding B & Yu J, Porous materials for sound absorption, *Compos Commun*, **10** (2018) 25–35.
- Arenas J & Crocker M, Recent Trends in porous sound-absorbing materials, *Sound Vib*, **44** (2010) 12–17.
- Fan M, Dai D & Huang B, Fourier transform infrared spectroscopy for natural fibers in fourier transform - Materials analysis, *Intech Open*, (2012) 45–68.

- 22 Khan M Z H, Sarkar M A R, Al Imam F I, Khan M Z H & Malinen R O, Paper making from banana pseudo-stem: Characterization and comparison, *J Nat Fibers*, **11** (2014) 199–211.
- 23 Bakri M K & Jayamani E, Comparative study of functional groups in natural fibers: Fourier Transform Infrared analysis (FTIR), *Int Conf Futuristic Trends Eng Sci, Human, Technol*, 23–24, January 2016, 167–174.
- 24 Petrov R H, García O L, Mulders J J L, Reis A C C, Bae J H, Kestens L & Houbaert Y, Three dimensional microstructure–microtexture characterization of pipeline steel, *Mater Sci Forum*, **550** (2007) 625–630.
- 25 Sathishkumar T P, Navaneethkrishnan P, Shankar S & Rajasekar R, Characterization of new cellulose *Sansevieria ehrenbergii* fibers for polymer composites, *Compos Interfaces*, **20** (2013) 575–593.
- 26 Singh P P & Nath G, Fabrication and analysis of luffa natural fiber based acoustic shielding material for noise reduction, *J Nat Fibers*, **19** (2022) 11218–11234.
- 27 Iqbal M N, Malek Mohd F, Lee Y S, Zahid L & Mezan M S, A study of the anechoic performance of rice husk-based, geometrically tapered, hollow absorbers, *Int J Antennas Propag*, **2014** (2014) 1–9.
- 28 Atmakuri A, Palevicius A, Janusas G & Eimontas J, Investigation of hemp and flax fiber-reinforced Eco Pox matrix biocomposites: morphological, mechanical, and hydrophilic properties, *Polymers*, **14** (2022) 4530–4551.
- 29 Burger N, Laachachi A, Ferriol M, Lutz M, Toniazzo V & Ruch D, Review of thermal conductivity in composites: Mechanisms, parameters and theory, *Prog Polym Sci*, **61** (2016) 1–28.
- 30 Tsekmes A, Kochetov R, Morshuis P & Smit J J, Thermal conductivity of polymeric composites: A Review, in *IEEE Int Conf Sol Dielectr ICSD* (Bologna, Italy) 30 June – 04 July 2013, 678–681.
- 31 Wang C, Zuo Q, Lin T, Anuar N I S, Mohd Salleh K, Gan S, Yousfani S H S, Zuo H & Zakaria S, Predicting thermal conductivity and mechanical property of bamboo fibers/polypropylene nonwovens reinforced composites based on regression analysis, *Int Commun Heat Mass Transf*, **118** (2020) 104895.
- 32 Gopinath A, Kumar M S & Elayaperumal A, Experimental investigations on mechanical properties of jute fiber reinforced composites with polyester and epoxy resin matrices, *Procedia Eng*, **97** (2014) 2052–2063.
- 33 Reddy B M, Mohana Reddy Y V, Mohan Reddy B C & Reddy R M, Mechanical, morphological, and thermogravimetric analysis of alkali-treated Cordia-Dichotoma natural fiber composites, *J Nat Fibers*, **17** (2020) 759–786.
- 34 Dong K & Wang X, Development of cost effective ultra-light weight cellulose-based sound absorbing material over silica sol/natural fiber blended substrate, *Carbohydr Polym*, **255** (2021) 117369.
- 35 Tan W & Sin C F, Sound transmission loss analysis on building materials, *Int J Automot Mech Eng*, **15** (2018) 6001–6011.
- 36 Singh V K & Mukhopadhyay S, Studies on the effect of hybridization on sound insulation of coir-banana-polypropylene hybrid biocomposites, *J Nat Fibers*, **19** (2022) 349–358.
- 37 Vinay C H, Goudanavar P & Acharya A, Development and characterization of pomegranate and orange fruit peel extract based silver nanoparticles, *J Manmohan Memorial Inst Health Sci*, **4** (2018) 72–85.
- 38 Asim M, Paridah M T, Chandrasekar M, Shahroze R M, Jawaid M, Nasir M & Siakeng R, Thermal stability of natural fibers and their polymer composites, *Iran Polym J*, **29** (2020) 625–648.
- 39 Sinha E & Rout S K, Influence of fiber-surface treatment on structural, thermal and mechanical properties of jute fiber and its composite, *Bull Mater Sci*, **32** (2009) 65–76.